Calculation of the replacement correction factors for ion chambers in megavoltage beams by Monte Carlo simulation

L. L. W. Wang[a] and D. W. O. Rogers[b]
Ottawa Carleton Institute of Physics, Carleton University Campus, Ottawa K1S 5B6, Canada

(Received 10 October 2007; revised 22 February 2008; accepted for publication 26 February 2008; published 11 April 2008)

This article describes four methods of calculating the replacement correction factor, P_{repl} (or the product $p_{cav}p_{dis}$ in the IAEA's notation), for a plane-parallel chamber in both electron and photon beams, and for a Farmer chamber in photon beams, by using the EGSnrc Monte Carlo code. The accuracy of underlying assumptions and relative merits of each technique are assessed. With careful selection of parameters it appears that all four methods give reasonable answers although the direct methods are more intellectually satisfying and more accurate in some cases. The direct methods are shown to have an accuracy of 0.1% when appropriate calculation parameters are selected. The depth dependence of P_{repl} for the NACP02 plane-parallel chamber has been calculated in both 6 and 18 MeV electron beams. At the reference depth ($0.6R_{50}-0.1$ cm) P_{repl} is 0.9964 for the 6 MeV beam and 1.0005 for the 18 MeV beam for this well-guarded chamber; at the depth of maximum dose for the 18 MeV beam, P_{repl} is 1.0010. P_{repl} is also calculated for the NACP02 chamber and a Farmer chamber (diameter 6 mm) at a depth of 5 cm in a ^{60}Co photon beam, giving values of 1.0063 and 0.9964, respectively. For the Farmer chamber, P_{repl} is about half a percent higher than the value (0.992) recommended by the AAPM dosimetry protocol. It is found that the dosimetry protocols may have adopted an incorrect value of P_{repl} for cylindrical chambers in photon beams. The nonunity values of P_{repl} for plane-parallel chambers in lower energy electron beams imply a variety of values used in dosimetry protocols must be reassessed. © *2008 American Association of Physicists in Medicine*. [DOI: 10.1118/1.2898139]

Key words: Prepl, fluence correction, clinical dosimetry protocols, Monte Carlo, EGSnrc

I. INTRODUCTION

In ion chamber dosimetry, the replacement correction factor P_{repl} accounts for the medium of interest being replaced by the air cavity of the chamber. In the AAPM's TG-21 dosimetry protocol,[1] $P_{repl}=P_{gr}P_{fl}$, where P_{gr} is the gradient correction and P_{fl} is the fluence correction (corresponding to the displacement perturbation p_{dis} and the fluence perturbation p_{cav}, respectively, in the IAEA's notation). It is conceptually difficult, if not impossible, to rigorously separate these two corrections since both are related to the effects of the cavity in the water phantom. Operationally one can treat P_{gr} as that part of the correction accounted for by an effective point of measurement, but, for example, P_{gr} in photon beam reference dosimetry is corrected for by a multiplicative factor and not a point of measurement shift. For plane-parallel chambers in electron beams, the effective point of measurement is taken at the center of the inner surface of the front wall and the gradient correction is assumed to be nonexistent; so P_{repl} is equal to P_{fl} (or p_{cav}). For well-guarded plane-parallel chambers in electron beams, P_{repl} is generally assumed to be unity in dosimetry protocols.[1–4] There were many experiments[5–10] done in the past to measure P_{repl} for some plane-parallel chambers in electron beams; but the results fluctuated as all the measurements had large (1%–2%) uncertainties. It will be very useful in clinical radiation dosimetry if one can calculate P_{repl} with high accuracy. Analytical methods of calculating P_{repl} in electron beams have been tried before as reviewed by Nahum,[11] but the results are not very satisfactory, especially for cylindrical chambers. As far as we know, the first Monte Carlo calculation of P_{repl} for plane-parallel chambers in electron beams was by Ma and Nahum[12] who used the EGS4 code. However, their results may have a systematic error of at least 0.5% due to the reasons discussed later. Both Buckley and Rogers[13] and Verhaegen *et al.*[14] used an indirect Monte Carlo method with EGSnrc (Ref. 15) to calculate P_{repl} for an NACP chamber (the method labeled SPR below). As discussed below, this is an indirect method which suffers from issues related to the selection of what energy threshold, Δ, to use when calculating the stopping-power ratios and makes the assumption that there is no change in the shape of the electron fluence spectrum in-phantom versus in the cavity. However, as we will show below by comparison to more direct methods, despite the uncertainties, this method does give reasonable results.

For cylindrical chambers in photon beams, P_{repl} represents a significant uncertainty in dosimetry protocols.[16] The AAPM's TG-51 (Ref. 2) and TG-21 (Ref. 1) dosimetry protocols use a value of $P_{repl}=0.992$ for a cylindrical chamber of inner diameter of about 6 mm in a ^{60}Co beam. This value is from the work of Cunningham and Sontag[17] who derived P_{repl} based on analytical calculations and experiments. For the same quantity the IAEA's TRS 398 (Ref. 4) and TRS 277 (Ref. 3) Codes of Practice use a value of 0.988 which is based on the measured data of Johansson *et al.*[18] This one half percent difference in the values used by the IAEA and

AAPM protocols may be the largest single difference between them, although in TG-51 and TRS-398, the differences have a reduced effect because only ratios of P_{repl} values are used. For plane-parallel chambers in megavoltage photon beams, P_{repl} is assumed to be unity in dosimetry protocols if the inner surface of the front wall is taken as the point of measurement. Boutillon[19] calculated analytically the P_{repl} value for the BIPM standard plane-parallel chamber at different depths in a graphite phantom irradiated by a ^{60}Co beam. For situations in which either the front face or the center of the cavity were taken as the point of measurement, she obtained values of 1.007 and 0.989, respectively, at a depth of 5 g/cm^2. Ferreira *et al.*[20] got the same results as Boutillon's by using the EGS4 Monte Carlo code to calculate the P_{repl} value for the same chamber under the same conditions.

In this article, we first present four different ways of calculating P_{repl} using the EGSnrc (Ref. 15) Monte Carlo code system and discuss their relative merits. Then we present calculated results, with high statistical precision (<0.1%), for an NACP02 plane-parallel chamber in a 6 MeV electron beam, an 18 MeV electron beam, and in a ^{60}Co beam, and for a Farmer chamber with a diameter of 6 mm in a ^{60}Co beam. With a proven method for calculating P_{repl} values for plane-parallel chambers, one may be able to partially explain why the nonunity values of P_{wall} reported recently[13,14,21] have not been previously noted experimentally. These methods can be used to reevaluate a wide range of prior ion chamber dosimetry studies since many of them were based on incorrect assumptions about values of P_{repl} and P_{wall}.

II. MATERIALS AND METHODS

II.A. Calculation methods

Using the Spencer–Attix formalism, the dose in a water phantom, D_{water}, is related to the dose in the air cavity, D_{air}, of a chamber with the point of measurement at the same location in the water phantom by

$$\frac{D_{water}}{D_{air}} = \left(\frac{\bar{L}_\Delta}{\rho}\right)^{water}_{air} P_{cel} P_{wall} P_{repl}, \quad (1)$$

where $(\bar{L}_\Delta/\rho)^{water}_{air}$ is the Spencer–Attix water/air mean restricted mass collision stopping-power ratio (SPR) with cutoff energy Δ, P_{cel} corrects for the central electrode being different from the cavity medium, and P_{wall} corrects for the chamber wall material being different from the medium. For a water-walled chamber with no central electrode

$$\frac{D_{water}}{D_{air}} = \left(\frac{\bar{L}_\Delta}{\rho}\right)^{water}_{air} P_{repl}. \quad (2)$$

Equation (2) gives an indirect method of calculating P_{repl} as the quotient of the ratio of the dose in the water phantom to that in the collecting volume of air cavity and the water/air SPR. The dose ratio and the SPR can be calculated, respectively, by the EGSnrc (Ref. 15) user-codes CAVRZnrc and SPRRZnrc, which were benchmarked before by Rogers and Kawrakow.[22] We will call this the SPR method.

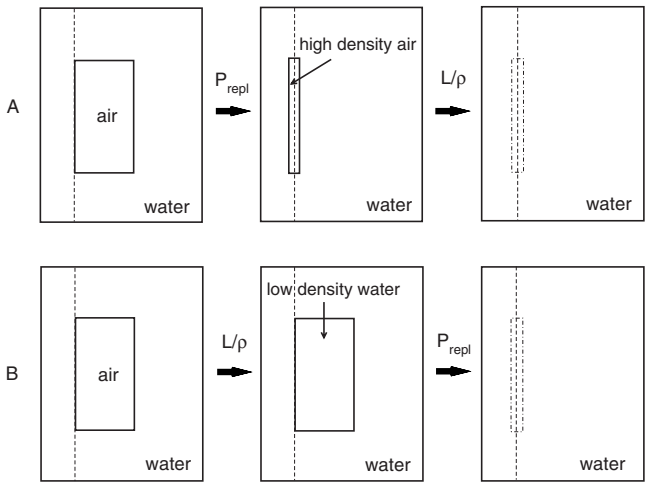

FIG. 1. Schematic diagram of two routes in calculating P_{repl} for a water-walled plane-parallel chamber in a water phantom. In route A, P_{repl} is calculated as the ratio of the dose in the HDA slab to that in air cavity. In route B, P_{repl} is calculated as the ratio of the dose in the water phantom to that in the LDW cavity. The dashed line indicates the depth of measurement in water.

Our goal is to calculate P_{repl} directly so that we can verify the accuracy of Eqs. (1) and (2). Figure 1 depicts the transition from the dose in an air cavity (first box) to the dose in a water phantom (third box), taking a plane-parallel chamber as an example (it is the same for a cylindrical chamber except the point of measurement is at the center of the cavity). Conceptually, the transition can be considered in two ways, either route A or route B as shown in Fig. 1. In route A, we put a thin slab of "high density air" (HDA) material centered at the point of measurement. Initially, we assume that the HDA slab does not affect the electron fluence spectrum compared to that in a pure water phantom. HDA is an artificial material that has all the dosimetric properties of normal air except its density is equal to that of water. In preparing the HDA data set, the density correction data for normal-density air is used. Dose is scored for the collecting volume of the air cavity (i.e., excluding the 3 mm guard ring) and the HDA slab in separate runs and P_{repl} is calculated as the ratio of these doses. We call this the HDA method. In route B, we replace air in the cavity by a "low density water" (LDW) material, which is water but with a density of normal air, and a density correction corresponding to normal-density water. The assumption here is that the electron fluence spectrum is the same in the collecting volume for both cavities. Both HDA and LDW methods avoid the stopping-power ratio in calculating P_{repl} as the materials involved have the same dosimetric properties except the density difference. We must keep in mind, however, that these two methods have approximations: HDA has a finite thickness of a different material from the medium so its presence may perturb the electron fluence and the LDW cavity is not air so the particle fluence in or near the cavity may be changed to some extent.

Originally, the HDA method was used by Ma and Nahum[12] in their calculation of P_{repl} for plane-parallel chambers. Ma and Nahum[23] also used a method similar to the

LDW method to calculate the displacement correction factor for cylindrical chambers in medium energy photon beams but it differs from our LDW method as they calculated the water kerma ratio as opposed to dose ratio and the kerma was averaged over the whole chamber volume.

If the electron spectrum in the cavity is very similar to that in the phantom at the point of measurement, P_{repl} can be approximated by the ratio of the total electron fluences in the cavity and phantom. Ma and Nahum[12] mentioned this approach but did not actually calculate it. The fourth (FLU) method of calculating P_{repl} calculates it as the ratio of the total electron fluence at the point of measurement in the phantom to the total electron fluence in the collecting volume of the cavity Φ_w/Φ_{cav}.

In this work, P_{repl} is calculated for a water-walled NACP02 plane-parallel chamber (2 mm in thickness, 8 mm in overall radius, and 5 mm collecting volume radius) at various depths in a water phantom irradiated by either a 6 or an 18 MeV electron beam, or at a depth of 5 cm irradiated by a ^{60}Co beam. P_{repl} is also calculated for a cylindrical air cavity (6 mm diameter, 2 cm length) corresponding to a Farmer chamber in a ^{60}Co beam at a phantom depth of 5 cm. Several EGSnrc user codes[24] have been employed for various purposes, including CAVRZnrc (for cavity dose in RZ geometry, see below), SPRRZnrc (for stopping-power ratios), FLURZnrc (for electron fluence and fluence spectra in RZ geometry), DOSRZnrc (for dose in a water phantom), and the new C++-based user-code Cavity (for dose calculation in Farmer chambers). We also implemented the ability to calculate the electron fluence in the Cavity code so that we can calculate the electron fluence in a thimble chamber with its axis perpendicular to the beam. It was necessary to run the Cavity code in double precision for calculations with small radii. For NACP02 chamber calculations, the RZ series of EGSnrc user codes are used. The cavity is put on the central axis of a cylindrically symmetric water phantom with a radius of 20 cm and a depth of 30 cm. The radiation source is at 100 cm source-surface-distance (SSD) for the electron beams and at 80 cm SSD for the ^{60}Co beam, with a field size of 5.6 cm radius (10×10 cm^2 equivalent). The cavity dose is only scored in the collecting volume of the chamber cavity, which has a radius of 0.5 cm. The point of measurement is at the proximal face of the cavity. For the Farmer chamber calculation, the phantom is a cube of 30 cm sides and the ^{60}Co source is at 80 cm SSD, 10×10 cm^2 field size. The point of measurement is at the center of the cylindrical cavity. The spectra of the incident electron beams are from a Monte Carlo simulation of a Varian Clinac 2100C linac.[25] For the 18 MeV electron beam, we also used a BEAMnrc simulation of a Clinac 2100C linac as the radiation source and compared the result to that of the spectrum source. The spectrum for the ^{60}Co calculations is from Mora *et al.*[26] When scoring doses or fluences at depths in the water phantom, for the standard RZ user codes, the voxel has a radius of 0.5 cm (i.e., corresponding to the collecting volume radius of the NACP02 chamber cavity); and for the Cavity calculations, the voxel has a radius of 1 cm (corresponding to the half length of a typical Farmer chamber). For both cases the thickness of the voxel is 0.2 mm which is chosen as a compromise between speed and accuracy, with the exception of the HDA method where we used thicknesses of 0.001 and 0.6 mm for the HDA slab.

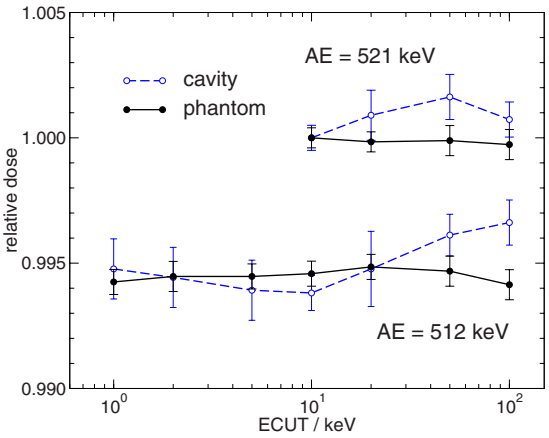

FIG. 2. Relative doses as a function of ECUT in the NACP02 cavity and in the phantom at depth R_{50} in the 6 MeV electron beam, for two different AE values. The doses are separately normalized in the cavity and the phantom at AE=ECUT=521 keV (10 keV kinetic energy).

II.B. Accuracy

II.B.1. Electron energy thresholds and cutoffs

EGSnrc is a class II Monte Carlo code for electron and photon transport[15] in which a secondary electron is explicitly simulated if the production energy is larger than a threshold, i.e., AE in EGSnrc. An electron's history is terminated if its energy falls below a cutoff energy, i.e., ECUT in EGSnrc. Obviously, the lower AE and ECUT are, the more accurate and also much longer the simulation is. For example, using AE=512 keV (total energy) is about 3–5 times slower than using AE=521 keV, even if the ECUT values are the same. As we are interested in 0.1% accuracy, we need to know how AE and ECUT can affect the calculation results. Two cross-section data sets were created and used in calculations with AE=512 keV and AE=521 keV. Radiation dose in the cavity of the NACP02 chamber is calculated, for varying ECUT for both AEs, at a depth of R_{50} in a 6 MeV electron beam. Dose is also calculated at the respective points of measurement in the water phantom with a scoring voxel size of 5 mm radius and 0.2 mm thickness. Figure 2 shows the calculated relative doses in the cavity and in the phantom at depth R_{50}, in a 6 MeV beam for different AEs and ECUTs. The calculation is done by the CAVRZnrc code. This figure shows that: (1) for a given AE and with a statistical uncertainty of 0.1% or less, the cavity and the phantom doses are almost independent of ECUT, ranging from 1 to 100 keV and (2) for either case, the dose calculated with AE=512 keV is about 0.5% lower than with AE=521 keV. This difference in the calculated dose is due to the difference in energy-loss straggling for different production thresholds for creating secondary electrons. We have calculated depth-dose curves with these two AE values and found that at R_{50} the dose with

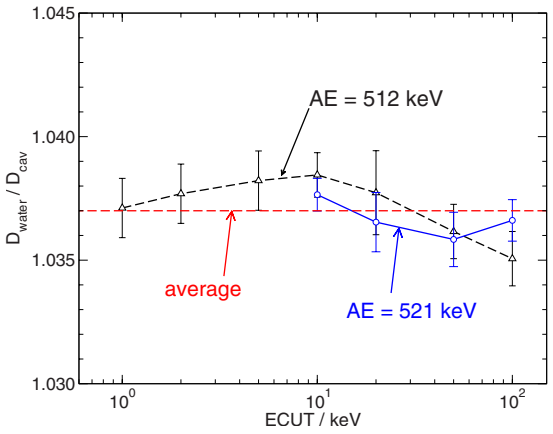

FIG. 3. The ratio of the phantom dose to the cavity dose vs ECUT for two AE values for the same case as Fig. 2.

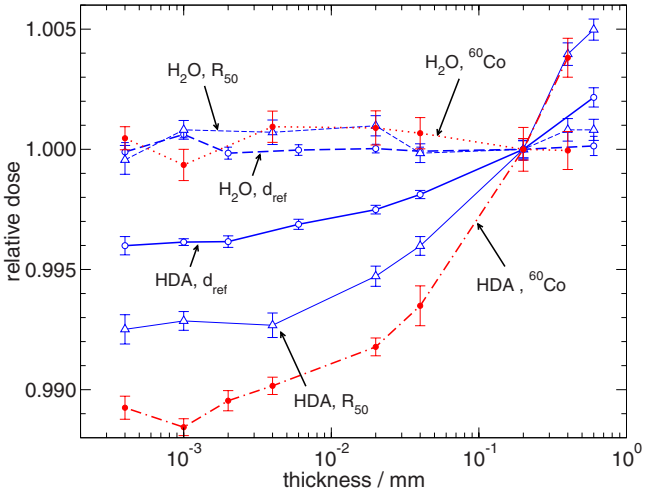

FIG. 4. Dose in a water slab and an HDA slab as a function of the slab thickness. The calculation is at d_{ref} and R_{50} in the 6 MeV electron beam and at depth 5 cm in the ^{60}Co beam. The doses are normalized at a slab thickness of 0.2 mm.

AE=512 keV is 0.5% lower than with AE=521 keV, confirming our expectation. In the falloff region of electron beam depth-dose curves the effect of energy-loss straggling is more pronounced because the electrons are nearing the end of their ranges. Calculated doses do not show much variation near the depth of maximum dose in the 6 MeV electron beam nor at a depth of 5 cm in a ^{60}Co photon beam. However, this energy-loss straggling effect is significant only if we are interested in absolute dose calculation. For a dose ratio calculation, such as P_{repl} in this work, the effect cancels. Figure 3 shows that the ratio of the phantom dose to the cavity dose is actually independent of AE and ECUT within calculation uncertainty of about 0.1%–0.2%, which justifies the use of AE=521 keV to save computing time. Similar calculations to that shown in Figs. 2 and 3 were also done for: (1) both an HDA slab of thickness of 1 μm and a water slab of the same thickness for different AE and ECUT values, at R_{50} in the 6 MeV beam, by the CAVRZnrc code and (2) a cylindrical cavity with a radius of 3 mm and a length of 2 cm at a depth of 5 cm in a ^{60}Co beam by the Cavity code. The results (not shown) demonstrate that for either the HDA/water dose ratio or the cylindrical cavity dose there is virtually no dependence (at the 0.1% level) on the ECUT and AE values from 1 to 20 keV.

II.B.2. Perturbation of the HDA slab and the LDW cavity

As mentioned earlier, the HDA method assumes the electron fluence spectrum is the same in the HDA and in the water. To check the validity of this assumption, the dose is calculated in the HDA slab and in the same slab with HDA being replaced by water, at a variety of slab thicknesses with the radius fixed at 5 mm, in both the 6 MeV electron beam (at d_{ref} and R_{50}) and the ^{60}Co beam (at a depth of 5 cm). Figure 4 shows that the dose to the water slab in a water phantom is independent of the slab thickness used (from 0.4 μm to 0.6 mm). However, for the HDA slab in the water phantom the dose varies significantly, indicating a non-negligible perturbation effect for thicker slabs, especially for the ^{60}Co beam and for the electron beam at R_{50}. One concludes that the HDA slab has to be very thin to make the perturbation effect negligible in the HDA. For electron beams the perturbation appears to be negligible for thickness of 2 μm or less and even in the ^{60}Co beam it is less than a 0.1% effect for a 1 μm thickness. A direct calculation of the electron fluence spectrum in the HDA slab and in the water phantom gives the results shown in Fig. 5. For an HDA slab thickness of 0.2 mm, there is a difference in the spectrum in the water phantom (solid line) and HDA slab (dashed line) for energies below 100 keV. However, when the HDA slab thickness decreases to 4 μm, the spectrum in the HDA (symbol ×'s) matches that for water as illustrated in the figure, indicating a negligible perturbation effect.

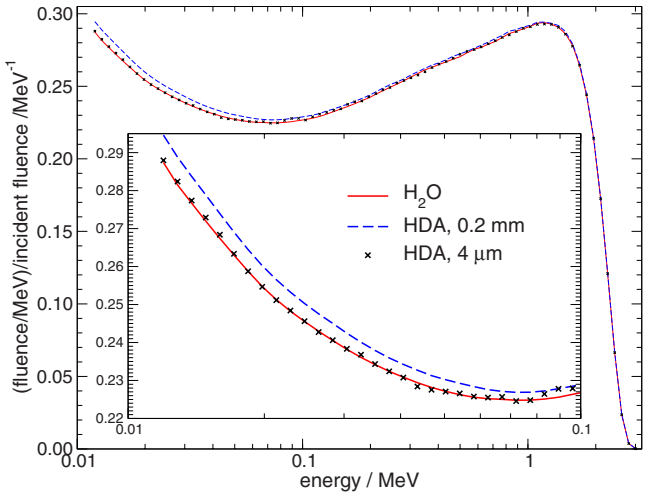

FIG. 5. Electron fluence spectra in a water slab (0.2 mm thick) and in HDA slabs of thicknesses of 0.2 and 0.004 mm. The calculation is at R_{50} in the 6 MeV electron beam. The inset shows the magnified portion of the curves from 10 to 100 keV. The spectra calculation uncertainty is about 0.2% or less.

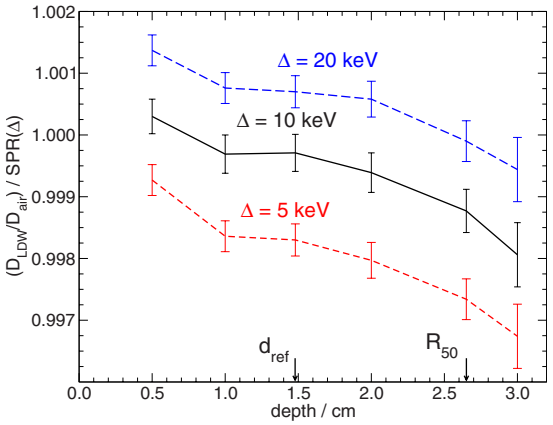

FIG. 6. Ratio of the dose ratio (low density water cavity to normal air cavity for NACP02 chamber) and the restricted water/air stopping power ratio for different Δ's as a function of depth in the 6 MeV electron beam.

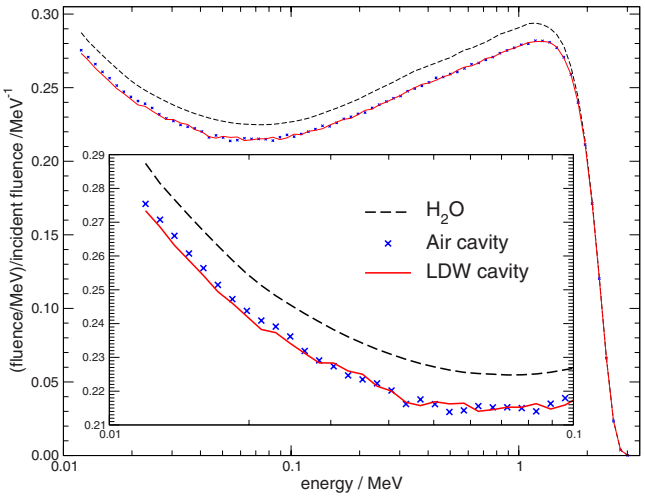

FIG. 7. Electron fluence spectra in a water phantom and in the collecting volume of the NACP02 chamber cavity filled with either air or LDW. The calculation is at R_{50} in the 6 MeV electron beam. The inset shows the magnified portion of the curves from 10 to 100 keV. The spectra calculation uncertainty is less than 0.4%.

For the LDW method, filling the cavity with LDW instead of air may perturb the electron fluence in the cavity. Ideally, if Spencer–Attix cavity theory holds and there is no perturbation of the electron fluence in the LDW filled cavity, we expect the ratio of the dose in the LDW cavity to that in the air cavity to be equal to the water/air SPR. To verify this, we calculated the ratio of the dose in the LDW cavity to that in the air cavity at various depths in the 6 MeV electron beam for the NACP02 chamber cavity and compared it to the water/air SPR at corresponding depths in the same beam. The water/air SPR is calculated with different values of Δ (5, 10, 20 keV) since the correct value is not well specified. Figure 6 presents the ratio of the two ratios as a function of depth, viz. $D_{\mathrm{LDW}}/D_{\mathrm{air}}$ for the NACP02 cavity, to $(\bar{L}/\rho)^{\mathrm{water}}_{\mathrm{air}}$ for the three Δ values. This ratio would be unity for an appropriately selected Δ if the difference in materials caused no fluence perturbation. Figure 6 shows that: (1) there is only a small fluence perturbation due to material difference; for a given value of Δ, the ratio varies less than 0.2% ($\sigma < 0.04\%$) from the surface to R_{50}, (2) the ratio varies with Δ but is not very sensitive to the value, varying less than 0.3% at a given depth for Δ ranging from 5 to 20 keV, and (3) for Δ=10 keV, near d_{ref}, the ratio is very close to unity, i.e., the 10 keV value of Δ commonly used in ion chamber dosimetry is a good choice at this depth. The slight decrease in the ratio with depth is consistent with the required value of Δ increasing with depth since the average path of an electron in the cavity increases with depth because of the increasing spread in angle of the electrons. Figure 7 shows the electron fluence spectra in the collecting volume of the chamber cavity, together with that in the water phantom. The symbol ×'s are the spectrum for the cavity filled with air and the solid line is for the cavity filled with LDW. The curves for air and LDW match everywhere except at energies lower than 30 keV where there might be a 0.5%–1% difference. This may explain point (1) listed above, i.e., a small fluence perturbation due to the difference in materials leads to the slight decrease of the ratio with depth. Another notable thing in Fig. 7 is that the spectrum in water differs from that in the cavity by approximately a constant ratio over almost the entire energy range.

II.C. Computation time

All the calculations for this work are performed on a cluster with 48 nodes and each node has four 3 GHz Intel Woodcrest cores. Table I lists the approximate time in hours to calculate P_{repl} by different methods for an 18 MeV electron beam for both a spectrum source and a BEAMnrc simulation source. The time listed is the total CPU time needed to calculate P_{repl} to a precision of 0.1%. There is a big difference between using a spectrum source and a simulation source. This is because a linac simulation takes a lot of time to generate a useful particle and most of these particles are photons (about 78%) which do not contribute much dose in the cavity. The other option is to generate and use a phase-space file. However, to get a cavity dose with a precision of 0.1% for the 18 MeV simulation source, one needs at least 8 billion particles which corresponds to a phase-space size of about 240 GB. This is beyond our capacity. Note the time listed for the simulation source is the longest possible time needed for the calculation since there is no particle reuse or

TABLE I. Comparison of the CPU time on an Intel Woodcrest 3 GHz core needed to calculate P_{repl} with a statistical uncertainty of 0.1% by the four methods for the NACP02 chamber cavity at $d_{\max}$ in an 18 MeV electron beam when using a spectrum source or a beam simulation source. For the HDA method, the HDA slab thickness is 1 μm.

	CPU time required (h)			
	SPR	HDA	LDW	FLU
Spectrum source	50	50	36	90
Simulation source	1600	4000	1500	-

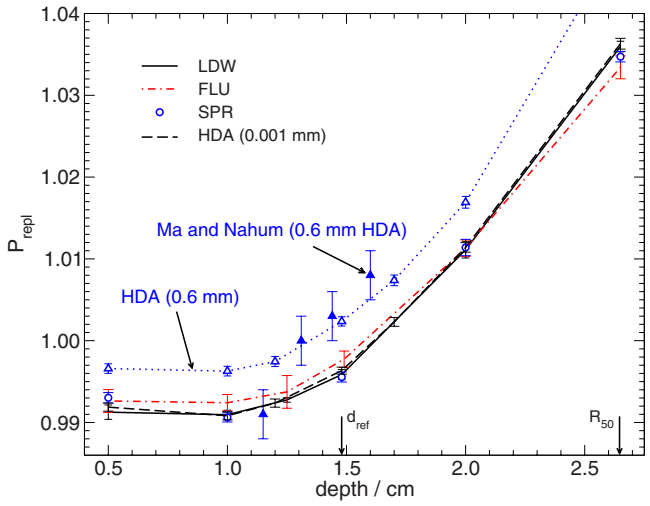

FIG. 8. P_{repl} values calculated by the four methods for the cavity of an NACP02 chamber as a function of depth in the 6 MeV electron beam. For the HDA method, the calculation is done for two HDA slab thicknesses, 0.6 mm (open triangle) and 0.001 mm (dashed line). Solid triangles were calculated with EGS4 by Ma and Nahum (Ref. 12), for an HDA thickness of 0.6 mm. Calculations are done with a spectrum source from Ding and Rogers (Ref. 25).

recycling capability in the current implementation of the linac simulation source (SOURCE 23 in the code). There is still room for efficiency improvement in the future. Another point that can be made from Table I is that the LDW method takes the least amount of time compared to other methods.

III. RESULTS AND DISCUSSION

III.A. P_{repl} for NACP02 chamber in electron beams

Figure 8 shows P_{repl} values calculated by the four methods for the NACP02 chamber as a function of depth in the 6 MeV electron beam. The statistical uncertainties are less than 0.1%. It is seen that all the methods (except HDA with 0.6 mm slab thickness) give the same values within the statistical uncertainty. This suggests that the shape of the electron fluence spectrum in the cavity is very close to that in the phantom since the FLU method is applicable (see Fig. 7). The solid triangles show P_{repl} values calculated with EGS4 by Ma and Nahum[12]; who used a monoenergetic 6 MeV electron beam and an HDA thickness of 0.6 mm, with a calculation uncertainty of 0.3%. Our results for the 0.6 mm HDA calculation agree with theirs within statistics. The figure makes clear that using an HDA thickness of 0.6 mm causes a systematic error of more than 0.5%, consistent with what is expected from the results of Fig. 4.

Figure 8 shows that at d_{ref} (which is basically d_{max} for this beam) P_{repl} is close, but not exactly equal, to unity for the well-guarded NACP02 chamber. The deviation is about 0.4%. At depths closer to the phantom surface, P_{repl} is even farther away from unity. The less-than-unity value of P_{repl} at depths less than just past d_{ref} partly compensates the greater-than-unity wall correction P_{wall} found for this chamber,[13] although past this depth both P_{wall} and P_{repl} are greater than unity. Table II lists P_{repl} values calculated by the four methods at d_{ref} in the 6 MeV electron beam. The four methods all agree within about 0.1% of the average value as long as an adequately thin (1 μm) HDA slab thickness is used. The values in Table II agree within statistics with the value (0.994) of Verhaegen *et al.*,[14] who calculated values for a 6 MeV beam from a Clinac 2300 linac by the SPR method with a calculation uncertainty of 0.2%.

Figure 9 shows three sets of calculated P_{repl} values for the NACP02 chamber in 18 MeV electron beams. Again we see good agreement between the LDW method and the SPR method at different depths. It is notable that for this higher energy electron beam P_{repl} is essentially unity from the phantom's surface to a depth beyond d_{ref}. Also shown are the results calculated by Verhaegen *et al.*[14] with the SPR method for a Clinac 2300 (digitized from Fig. 6 in their article). It is seen there is a significant discrepancy at some depths, especially at d_{ref}. Verhaegen *et al.* used a phase-space file as the radiation source as opposed to our spectrum source. To find out if this causes any differences, we used a BEAMnrc linac simulation of the 18 MeV electron beam as the radiation source, as well as a spectrum source extracted from the 18 MeV electron beam modeling, and calculated P_{repl} at d_{ref} and d_{max} by the SPR, HDA, and LDW methods. The results show that the P_{repl} value calculated using the linac model agrees with that for a spectrum source within the calculation uncertainty of 0.1%. A similar calculation with a 22 MeV

TABLE II. Comparison of calculated P_{repl} values using four methods for the NACP02 chamber cavity at d_{ref} (close to d_{max}) in a 6 MeV, at both d_{ref} and d_{max} in an 18 MeV electron beams, and at 5 cm depth in a ^{60}Co beam. Also listed is the result for a Farmer chamber cavity (6 mm diameter, 2 cm length) at 5 cm depth in a ^{60}Co beam. For the HDA method in all the cases, the HDA slab thickness is 1 μm.

	SPR	HDA	LDW	FLU	Average
NACP02 in 6 MeV ($d_{ref} \approx d_{max}$)	0.9956 ± 0.06%	0.9963 ± 0.04%	0.9959 ± 0.06%	0.9977 ± 0.1%	0.9964
NACP02 in 18 MeV (d_{ref})	1.0001 ± 0.06%	1.0007 ± 0.06%	1.0005 ± 0.05%	1.0007 ± 0.06%	1.0005
NACP02 in 18 MeV (d_{max})	1.0004 ± 0.07%	1.0016 ± 0.07%	1.0010 ± 0.07%	1.0015 ± 0.06%	1.0011
NACP02 in ^{60}Co	1.0059 ± 0.1%	1.0066 ± 0.1%	1.0065 ± 0.1%	1.0063 ± 0.1%	1.0063
Farmer in ^{60}Co	0.9963 ± 0.08%	0.9969 ± 0.09%	0.9974 ± 0.07%	0.9952 ± 0.08%	0.9964

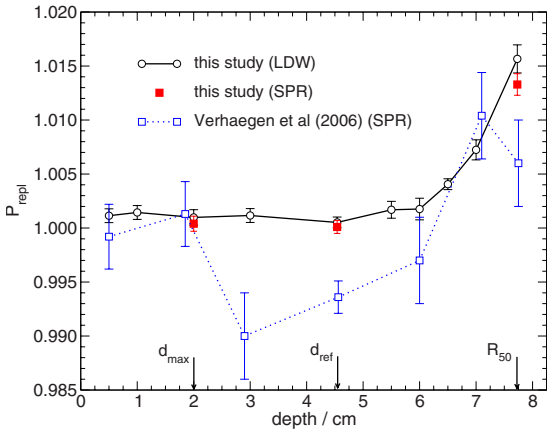

FIG. 9. P_{repl} values for the NACP02 chamber cavity as a function of depth in an 18 MeV electron beam [spectrum source for Varian Clinac 2100 from Ding and Rogers (Ref. 25)]. Open circles are the results for the LDW method and solid squares for the SPR method. Open squares are the results calculated by Verhaegen *et al.* (Ref. 14) with the SPR method for a Clinac 2300 beam with the same energy and the same R_{50}=7.73 cm as our Clinac 2100 model.

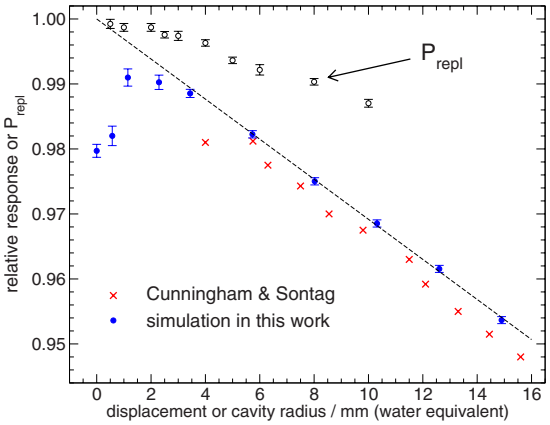

FIG. 10. Experimental measurements used by Cunningham and Sontag (Ref. 17) (×) to determine the displacement correction in a ^{60}Co beam. Our Monte Carlo simulation of their measurements are shown as filled circles. Dashed line is the linear fit (normalized to unity for 0 radius) for the simulation data points that have a displacement larger than 0.4 g/cm^2. Open circles are the values of P_{repl} for a cylindrical cavity of length 2 cm as a function of the cavity radius, calculated by the LDW method.

electron beam gives the same result. These results show that the high level of photon contamination, which is the major difference between a spectrum source and a simulation source, has little effect on the P_{repl} calculation.

III.B. P_{repl} for chambers in ^{60}Co photon beam

The P_{repl} values calculated by the four methods for the NACP02 chamber and the Farmer chamber at a depth of 5 cm in a ^{60}Co beam are listed in the fourth and fifth rows, respectively, in Table II. Dosimetry protocols assume a unity P_{repl} for all plane-parallel chambers in megavoltage photon beams, when the inner front face of the cavity is taken as the point of measurement. Our results disagree with the assumption by 0.6% for the NACP02 chamber. A calculation of the PDD curve for a ^{60}Co beam gives a dose gradient of about 0.6%/mm at a depth of 5 cm. Since the thickness of the air cavity is 2 mm, this suggests that the point of measurement for the NACP02 chamber in a ^{60}Co beam should be taken as the center of the air cavity of the chamber, as is done for these chambers in low and medium energy x-ray beams.[27] Since plane-parallel chambers are generally not recommended to be used in photon beams,[28] there are no experimental data available for the values of P_{repl} for plane-parallel chambers in photon beams. Although different chambers and phantoms are being studied, our results are consistent with those of Ferreira *et al.* and Boutillon mentioned in the Sec. I in that a greater-than-one value of P_{repl} is obtained if the front face of the air cavity for a plane-parallel chamber is taken as the point of measurement in a ^{60}Co beam.

For the Farmer chamber, the AAPM TG-21 dosimetry protocol[1] recommended a P_{repl} value of ~0.992 for a 6 mm diameter cavity in a ^{60}Co beam. Our results show a significant difference between P_{repl} used in the dosimetry protocol and that calculated by the Monte Carlo method which is closer to one. As mentioned earlier, the AAPM value of P_{repl} for a Farmer chamber in photon beams is based on the work of Cunningham and Sontag.[17] In one of their measurements for P_{repl}, which was called a displacement correction, a Farmer chamber was put at about 5 cm depth in the center of a hole with a diameter of 3.2 cm and a length of 2.5 cm in a Lucite phantom. The response was measured as a series of Lucite sleeves was added until the hole was completely filled up. The relative response of the chamber in a ^{60}Co beam was recorded and the results were plotted as a function of the water equivalent outer radius of the sleeves. Then, a linear regression was done to extrapolate the curve to zero radius, where the chamber response was normalized to 1. Their experimental results are shown in Fig. 10 as cross symbols. The figure also shows (open circles) the cavity radius dependence of P_{repl} calculated by the LDW method for a cylindrical cavity with a length of 2 cm. Note that P_{repl} approaches 1 as the cavity radius decreases to 0, as is expected. There is, however, an apparent discrepancy between the calculated P_{repl} and the experimental results, even the slopes at the linear part of the curve are different. To investigate this further, we used the Cavity code to simulate the actual experiment: an ion chamber with an air cavity with a diameter of 6 mm and a length of 2.5 cm with variable wall thickness is put in a hole (filled with air) with a diameter of 3.2 cm and a length of 2.5 cm, which is located at a 5 cm depth in a polymethylmethacrylate (PMMA) phantom irradiated by a ^{60}Co beam. The wall material is also PMMA and the dose in the air cavity, which is proportional to the chamber response, is scored while the wall thickness is gradually increased to fill the entire hole. A linear regression is done for data points where the wall thickness is greater than 0.4 g/cm^2 and the data points are normalized at the extrapolated zero wall thickness. These simulation results are represented by the solid circles and dashed line in Fig. 10. It is seen that the agreement of the simulation results with the measurement is excellent. The distinction between our P_{repl} calculation and

TABLE III. Calculated P_{repl} values (LDW method) for different cavity lengths for an ion chamber with diameter 6 mm (Farmer chamber) at 5 cm depth in an 80 cm SSD, 10×10 cm^2 ^{60}Co beam.

Cavity length (mm)	5	10	20
P_{repl}	$0.9953\pm0.06\%$	$0.9963\pm0.06\%$	$0.9974\pm0.07\%$

the simulation of the experiments demonstrates that the original interpretation of the experimental results in terms of P_{repl} is incorrect. Cunningham and Sontag[17] conceded that their interpretation was part of an on-going controversy. In retrospect, it was inappropriate for both the TG-21 (Ref. 1) and TG-51 (Ref. 2) protocols to interpret these measurements and calculations which were about kerma as being related to P_{repl} which concerns the change in the electron fluence spectrum.

Dosimetry protocols also assume P_{repl} does not depend upon the cavity length of cylindrical chambers in photon beams. To verify this assumption, we calculated P_{repl} in a ^{60}Co beam for a cylindrical cavity with a diameter of 6 mm and cavity lengths of 0.5, 1, and 2 cm. The results in Table III indicate a 0.2% effect as the length varies from 0.5 to 2 cm. This is barely statistically significant.

IV. CONCLUSIONS

In this work, Monte Carlo methods of calculating the replacement correction factors for ion chamber dosimetry have been investigated thoroughly for the first time. Four methods have been discussed and used to calculate P_{repl} for an NACP02 plane-parallel chamber at various depths in a 6 MeV electron beam and for a Farmer chamber of 6 mm diameter at 5 cm depth in a ^{60}Co beam. Two direct methods of calculation (HDA and LDW methods) have an accuracy of about 0.1%. For the HDA method, the HDA slab must be ≤1 μm thick. The two more indirect methods (SPR and FLU) appear to be accurate as well but introduce larger uncertainties related to uncertainties in the selection of Δ for the SPR method or the assumption of no change in the fluence spectrum for the FLU method. It is found that all four methods give almost the same P_{repl} values for an NACP02 plane-parallel chamber in either electron or photon beams and for a Farmer chamber in a photon beam. It should be noted that, for a Farmer chamber in electron beams, the calculation of P_{repl} becomes more complicated. This issue will be addressed separately.

The Monte Carlo calculated value of P_{repl} for the well-guarded NACP02 chamber at the reference depth in a 6 MeV electron beam is found to be 0.9964, which is lower than unity and partly compensates for the 1.7% above-unity wall correction factor for this chamber at the same depth.[13] In an 18 MeV electron beam, P_{repl} is found to be very close to unity ($1.0005\pm0.05\%$) at the reference depth for this chamber. In a ^{60}Co photon beam, P_{repl} for the NACP02 chamber is found to be 0.6% higher than unity, indicating the point of measurement might need to be at the center of the cavity for plane-parallel chambers as opposed to the assumptions in dosimetry protocols. For a Farmer chamber in a ^{60}Co beam, P_{repl} is 0.9964, which is about 0.4% higher than the value recommended or used by the AAPM dosimetry protocols and 0.8% larger than used in the IAEA Codes of Practice. This discrepancy is likely due to a misinterpretation of the calculations and measurements by Cunningham and Sontag[17] as used by TG-21 (Ref. 1) and TG-51 (Ref. 2). The fact that the direct and indirect methods of calculating P_{repl} agree with each other means that the present calculations are properly interpreted and the P_{repl} values calculated are correct.

For electron beam dosimetry, all experimental measurements of P_{repl} values have an uncertainty of 1%–2% and most of the measurements actually give the value of ratio of the product $P_{wall}P_{repl}$ for two different ion chambers. Values of P_{repl} are then extracted by making the assumption that P_{wall} is unity in electron beams and P_{repl} is unity for the reference chamber (typically the NACP). Both of these assumptions have now been shown to be incorrect. Thus, P_{repl} is a significant source of uncertainty in electron beam dosimetry. Now that accurate methods for calculating P_{repl} have been established, and given the previous work on P_{wall} factors, there is an opportunity to reassess many of the values used in routine clinical dosimetry and pave the way for the development of more accurate dosimetry protocols in the future.

ACKNOWLEDGMENTS

We wish to thank Alan Nahum for helpful comments on the manuscript. We thank the members of the Carleton Laboratory for Radiotherapy Physics, especially Dan LaRussa, for reading and making comments on the manuscript. This work has been supported by NSERC, the Canada Research Chairs program, CFI, and OIT.

[a]Electronic mail: lwang@physics.carleton.ca
[b]Electronic mail: drogers@physics.carleton.ca

[1]AAPM TG–21, "A protocol for the determination of absorbed dose from high-energy photon and electron beams," Med. Phys. **10**, 741–771 (1983).
[2]P. R. Almond, P. J. Biggs, B. M. Coursey, W. F. Hanson, M. S. Huq, R. Nath, and D. W. O. Rogers, "AAPM's TG–51 protocol for clinical reference dosimetry of high-energy photon and electron beams," Med. Phys. **26**, 1847–1870 (1999).
[3]IAEA, *Absorbed Dose Determination in Photon and Electron Beams: An International Code of Practice*, Technical Report Series Vol. 277 (IAEA, Vienna, 1987).
[4]IAEA, *Absorbed Dose Determination in External Beam Radiotherapy: An International Code of Practice for Dosimetry Based on Standards of Absorbed Dose to Water*, Technical Report Series Vol. 398 (IAEA, Vienna, 2001).
[5]H. Kubo, L. J. Kent, and G. Krithivas, "Determination of N_{gas} and P_{repl} factors from commercially available parallel-plate chambers," Med. Phys. **13**, 908–912 (1986).
[6]F. W. Wittkämper, H. Thierens, A. Van der Plaetsen, C. de Wagter, and B. J. Mijnheer, "Perturbation correction factors for some ionization chambers commonly applied in electron beams," Phys. Med. Biol. **36**, 1639–1652 (1991).
[7]F. T. Kuchnir and C. S. Reft, "Experimental values for $P_{wall,x}$ and $P_{repl,E}$ for five parallel-plate, ion chambers—A new analysis of previously published data," Med. Phys. **19**, 367 (1992).
[8]A. Van der Plaetsen, J. Seuntjens, H. Thierens, and S. Vynckier, "Verification of absorbed doses determined with thimble and parallel-plate ionization chambers in clinical electron beams using ferrous sulphate dosimetry," Med. Phys. **21**, 37–44 (1994).
[9]G. X. Ding and J. Cygler, "Measurement of $P_{repl}P_{wall}$ factors in electron

beams and in a ^{60}Co beam for plane-parallel chambers," Med. Phys. **25**, 1453–1457 (1998).
[10]C. S. Reft and F. T. Kuchnir, "Measured overall perturbation factors at depths greater than d_{max} for ionization chambers in electron beams," Med. Phys. **26**, 208–213 (1999).
[11]A. E. Nahum, "Perturbation effects in dosimetry: Part I. Kilovoltage x-rays and electrons," Phys. Med. Biol. **41**, 1531–1580 (1996).
[12]C.-M. Ma and A. E. Nahum, "Plane-parallel chambers in electron beams: Monte Carlo findings on perturbation correction factor," in *Proceedings of the IAEA International Symposium on measurement assurance in dosimetry* (IAEA, Vienna, 1994), pp. 481–493 (1994).
[13]L. A. Buckley and D. W. O. Rogers, "Wall correction factors, P_{wall}, for parallel-plate ionization chambers," Med. Phys. **33**, 1788–1796 (2006).
[14]F. Verhaegen, R. Zakikhani, A. DuSautoy, H. Palmans, G. Bostock, D. Shipley, and J. Seuntjens, "Perturbation correction factors for the NACP-02 plane-parallel ionization chamber in water in high-energy electron beams," Phys. Med. Biol. **51**, 1221–1235 (2006).
[15]I. Kawrakow and D. W. O. Rogers, "The EGSnrc Code System: Monte Carlo simulation of electron and photon transport," Technical Report No. PIRS–701, National Research Council of Canada, Ottawa, Canada, 2000.
[16]D. W. O. Rogers, in *Teletherapy Physics, Present and Future*, edited by J. R. Palta and T. R. Mackie (AAPM, Washington, DC, 1996), pp. 319–356.
[17]J. R. Cunningham and M. R. Sontag, "Displacement corrections used in absorbed dose determinations," Med. Phys. **7**, 672–676 (1980).
[18]K. A. Johansson, L. O. Mattsson, L. Lindborg, and H. Svensson, "Absorbed-dose determination with ionization chambers in electron and photon beams having energies between 1 and 50 MeV," IAEA Symposium Proceedings, Vienna, 1977, pp. 243–270.
[19]M. Boutillon, "Perturbation correction for the ionometric determination of absorbed dose in a graphite phantom for ^{60}Co gamma rays," Phys. Med. Biol. **28**, 375–388 (1983).
[20]I. H. Ferreira, A. Bridier, C. E. de Almeida, D. Marre, and J. Chavaudra, "Perturbation corrections for flat and thimble-type cylindrical standard ionization chambers for 60Co gamma rays: Monte Carlo calculations," Phys. Med. Biol. **43**, 2721–2727 (1998).
[21]L. A. Buckley and D. W. O. Rogers, "Wall correction factors, P_{wall}, for thimble ionization chambers," Med. Phys. **33**, 455–464 (2006).
[22]D. W. O. Rogers and I. Kawrakow, "Monte Carlo calculated correction factors for primary standards of air-kerma," Med. Phys. **30**, 521–543 (2003).
[23]C.-M. Ma and A. E. Nahum, "Calculations of ion chamber displacement effect corrections for medium-energy x-ray dosimetry," Phys. Med. Biol. **40**, 45–62 (1995).
[24]D. W. O. Rogers, I. Kawrakow, J. P. Seuntjens, B. R. B. Walters, and E. Mainegra-Hing, "NRC User Codes for EGSnrc," Technical Report No. PIRS–702(RevB), National Research Council of Canada, Ottawa, Canada, 2003.
[25]G. X. Ding and D. W. O. Rogers, Energy spectra, angular spread, and dose distributions of electron beams from various accelerators used in radiotherapy, National Research Council of Canada Report No. PIRS-0439, 1995; see http://www.irs.inms.nrc.ca/inms/irs/papers/PIRS439/pirs439.html.
[26]G. M. Mora, A. Maio, and D. W. O. Rogers, "Monte Carlo simulation of a typical ^{60}Co therapy source," Med. Phys. **26**, 2494–2502 (1999).
[27]C.-M. Ma, C. W. Coffey, L. A. DeWerd, R. Nath, C. Liu, S. M. Seltzer, and J. Seuntjens, "AAPM protocol for 40–300 kV x-ray beam dosimetry in radiotherapy and radiobiology," Med. Phys. **28**, 868–893 (2001).
[28]IAEA, *The Use of Plane Parallel Ionization Chambers in High Energy Electron and Photon Beams: An International Code of Practice for Dosimetry*, Technical Report Series Vol. 381 (IAEA, Vienna, 1997).